Electrical Power and Energy Systems 130 (2021) 106911

Contents lists available at ScienceDirect

International Journal of Electrical Power and Energy Systems

journal homepage: www.elsevier.com/locate/ijepes

Multiple blanking preprocessors for impulsive noise mitigation in OFDM-based power-line communication systems

Angie A.G. Liong [a], Filbert H. Juwono [a,*], Lenin Gopal [a], Choo W.R. Chiong [a], Yue Rong [b]

[a] Department of Electrical and Computer Engineering, Curtin University Malaysia, Miri, Sarawak 98009, Malaysia
[b] School of Electrical Engineering, Computing and Mathematical Sciences, Curtin University, Bentley, WA 6102, Australia

ARTICLE INFO

Keywords:
OFDM
PLC
MRC
Impulsive noise
Blanking

ABSTRACT

Power-line communication (PLC) technology has been a critical enabler for smart grid systems. It provides two-way communication links without new infrastructure deployment. However, as the power-line was not designed to carry data, there are many drawbacks when it is used as a communication channel. One of the major drawbacks is impulsive noise occurrence. Blanking nonlinear preprocessor has been commonly used for mitigating impulsive noise in orthogonal frequency-division multiplexing (OFDM)-based PLC. It uses a threshold to detect whether a signal sample is contaminated by impulsive noise. Optimum performance is obtained when the optimal blanking threshold is used. The optimal blanking threshold depends on noise parameters, which are usually assumed to be available to the receiver. However, they may not be known in practice. In this paper, we propose a blanking preprocessor bank consisting of multiple blanking preprocessors with different thresholds which blindly handles the impulsive noise. Each blanking preprocessor is considered to provide an independent channel. The output of all preprocessors is combined using the maximal ratio combining (MRC) technique at the OFDM demodulator. Simulation results show that the proposed blanking preprocessor bank method results in better performance compared to the one using the optimal threshold method.

1. Introduction

A smart grid refers to advanced electricity grid equipped with energy distribution management system which incorporates two-way information and communication technology, sensors, and control mechanism [1,2]. The applications of smart grid include remote fault detection, automatic meter reading (AMR), and vehicle-to-grid communications [3,4]. The smart grid utilizes both wireless and wireline technologies to transmit two-way communication data. Among wireline technologies, power-line communication (PLC) has been preferred to provide low-cost and reliable communication links as power-lines have been deployed widely [5]. Existing PLC standards have been classified as narrowband PLC (NB-PLC) operating in the 3–500 kHz frequency range and broadband PLC (BB-PLC) operating in the 1.8–86 MHz frequency spectrum [6].

As a power-line was not designed to transmit high-frequency data, it suffers from frequency-selective fading and noise problems [7,8]. Frequency-selective fading is caused by multiple branches of the power-lines and impedance mismatches. On the other hand, noise in the power-line cannot be modeled as a simple additive white Gaussian noise (AWGN) due to the presence of power converters and electrical components. In particular, the noise in PLC consists of background, narrowband, and impulsive noise [9]. Both background noise and narrowband noise have a slowly changing root mean square (RMS) amplitude so that they are usually combined and modeled as AWGN [10,11]. In contrast, the RMS amplitude of impulsive noise changes rapidly in a short duration, and its occurrence is random. It is common to model impulsive noise as a Bernoulli-Gaussian random process [12] in BB-PLC and cyclostationary random process in NB-PLC [13,14].

Multicarrier modulation techniques have been proposed for PLC. Besides Discrete Fourier transform (DFT)-orthogonal frequency-division multiplexing (OFDM), wavelet transform (WT)-OFDM has been proposed to overcome the impairments in PLC systems [15,16]. Although OFDM is well known to work well in multipath fading, it is not powerful enough to tackle the impulsive noise in PLC systems, thereby leading to performance degradation. This paper focuses on DFT-OFDM-based (or simply 'OFDM-based') BB-PLC.

A number of techniques have been proposed by researchers to minimize the effects of impulsive noise. In the literature, they can be grouped into threshold-based, compressive sensing-based, and hybrid techniques [17]. The threshold-based techniques include nonlinear preprocessing and iterative methods. In the threshold-based techniques,

* Corresponding author.

https://doi.org/10.1016/j.ijepes.2021.106911
Received 22 August 2020; Received in revised form 24 January 2021; Accepted 5 February 2021

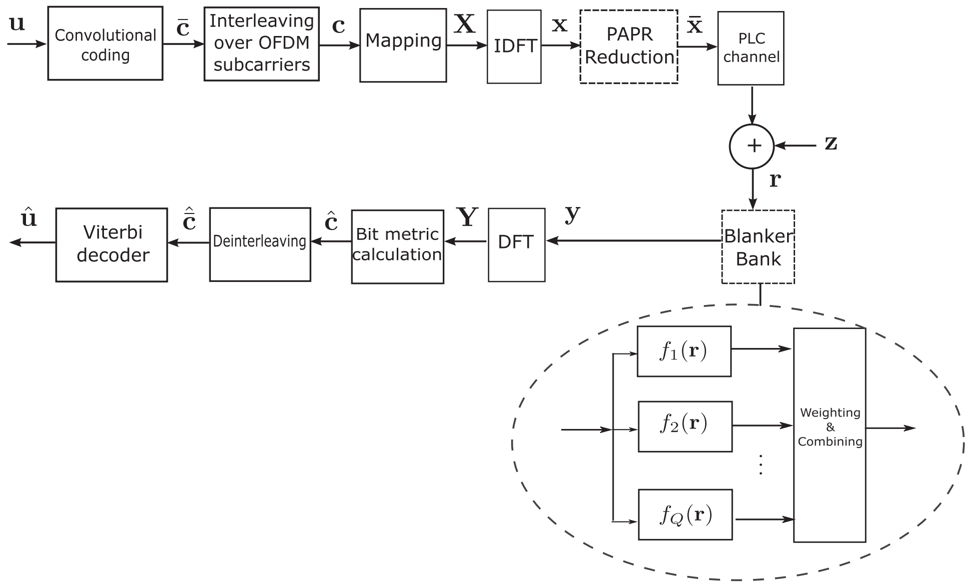

Fig. 1. System Model.

any samples exceeding the threshold are considered to be contaminated by impulsive noise, and they are treated according to the nonlinear function. The nonlinear preprocessing methods include clipping, blanking, joint blanking/clipping, deep clipping [18], and adaptive joint blanking/clipping methods [19]. To further improve the performance of the nonlinear preprocessing method, iterative methods, such as the methods presented in [20,21], can be employed. In addition to the nonlinear preprocessor method, the iterative method can be combined with an artificial neural network, as proposed in [22]. Compressive sensing-based technique uses null-subcarriers of the OFDM symbol to reconstruct the sparse impulsive noise. The reconstructed impulsive noise is then removed from the received signal. Algorithms for impulsive noise reconstruction available in the literature include, among others, smoothed-ℓ_0 (SL0) [23], sparse Bayesian learning [13], and multiple signal classification (MUSIC) [8]. Finally, the hybrid method combines the threshold-based and compressive sensing techniques, such as the one proposed in [24].

In this paper, the blanking nonlinear preprocessors are used since they have the simplest characteristic and have been used in many works. In [25], the blanking function was employed in the dynamic peak-based threshold estimation (DPTE) scheme in PLC. In [26], the performance of blanking nonlinearity in the real-valued OFDM-PLC system was derived and analyzed. In [27], the blanking nonlinear preprocessor was employed in the precoded OFDM-based PLC. In [28], a relation between signal power and blanking threshold in OFDM-based PLC was presented.

In order to obtain optimal performance, an optimal threshold needs to be obtained. It is worth mentioning that an incorrect threshold may lead to significant performance degradation [29]. Getting the optimal threshold of a blanking nonlinear preprocessor is not an easy task as the optimal threshold depends on the impulsive noise parameters [26]. Therefore, it is common to assume that the noise parameters are available to the receiver, which is not practical. Alternatively, we can estimate the noise parameters at the receiver [14]. Another approach to getting the reliable performance of blanking nonlinear preprocessor without estimating the noise parameters is to use the information from the received signal as proposed in [20]. However, the scheme in [20] involves a complex structure that employs feedback loops and requires additional computation for getting the received signal properties.

This paper proposes a simple blanking preprocessor bank consisting of multiple blanking preprocessors with different thresholds which can handle the impulsive noise without prior noise information. The individual output from each preprocessor is then weighted and combined. The thresholds should be carefully predetermined to make the system perform satisfactorily. Further, as OFDM signals have a large peak-to-average power ratio (PAPR), the blanking nonlinear preprocessor may falsely detect the impulsive noise. Some works have proposed to use the PAPR reduction technique to reduce the false alarms. In [30], selective mapping (SLM) was used as the PAPR reduction technique to reduce false alarm of blanking nonlinearity in PLC. Similarly, an extended SLM was used as the PAPR reduction technique in [31]. In [32], the effect of PAPR reduction and blanking threshold was analyzed. In this paper, we will also evaluate the effect of the PAPR reduction technique on the system performance. Here, we adopt the clipping method used in [33], which will not deteriorate the bit error rate (BER) performance, as the PAPR reduction technique.

The selection of threshold values affects the instantaneous output signal-to-noise ratio (SNR) of the blanking preprocessor bank, which will be analyzed using outage probability. On the other hand, the BER performance of the blanking preprocessor bank is better compared with the one using the optimal blanking preprocessor. Our contributions are summarized as follows:

1. We propose a blind blanking nonlinearity scheme where the optimal threshold is not required to be predetermined.
2. We evaluate the effects of the PAPR reduction on the performance of our proposed scheme.
3. We compare our proposed system with the one using the SL0 technique.

The rest of this paper is organized as follows. Section II discusses the system model, including the noise model and the proposed blanking preprocessor bank. Section III presents the simulation results and discussion. Finally, Section IV concludes this paper.

2. System model

We adopt a bit-interleaved coded modulation (BICM) scheme for OFDM-based PLC system, as shown in Fig. 1 [34]. Information sequence $\mathbf{u} = \{0,1\}$ is generated and passed to a convolutional encoder to obtain a codeword $\bar{\mathbf{c}}$, where $\bar{\mathbf{c}} \in \mathcal{C}$ and $\mathcal{C}$ is the coding scheme defined over $\{0,1\}$. A constellation set, $\mathcal{X}$, of size 2^m is used. A random ideal interleaver is

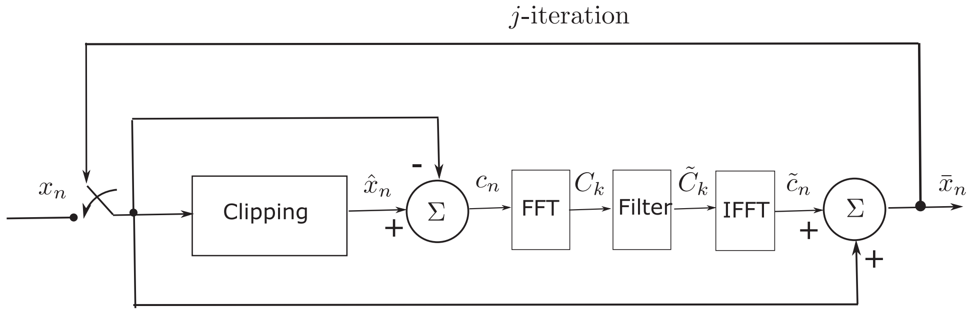

Fig. 2. Peak amplitude clipping.

applied to interleave the codeword over N OFDM subcarriers. Among N subcarriers, only K subcarriers are used to carry data, and $N-K$ subcarriers are nulled.[1] The interleaved codeword is given by

$$\mathbf{c} = \left[c_{0,1}, c_{0,2}, \cdots, c_{k,u}, \cdots, c_{N-1,m}\right], \tag{1}$$

where $c_{k,u}$ is the coded bit at the u-th label ($u = 1, \cdots, m$) of the k-th subcarrier. The coded bits are then mapped by the M-QAM or M-PSK modulator, where $M = 2^m$ as mentioned previously. The modulated signal vector, $\mathbf{X} = [X_0, \cdots, X_k, \cdots, X_{N-1}]^T$, where $(\cdot)^T$ denotes the transpose operation, is then formed to OFDM signal, $\mathbf{x} = [x_0, \cdots, x_n, \cdots, x_{N-1}]^T = \mathbf{F}^H\mathbf{X}$, where $\mathbf{F}$ is the DFT unitary matrix and $(\cdot)^H$ denotes the Hermitian operator. As a result, the OFDM signal can be expressed as

$$x_n = \frac{1}{\sqrt{N}} \sum_{k=0}^{N-1} X_k e^{j2\pi nk/N}. \tag{2}$$

A PAPR reduction technique may be applied to the OFDM signal before being appended by a cyclic prefix (not shown in the figure). The cyclic prefix is used to overcome intersymbol interference (ISI). Without loss of generality, we assume that the transmit power is unity. After removing the cyclic prefix at the receiver, the received signal, $\mathbf{r} = [r_0, \cdots, r_n, \cdots, r_{N-1}]^T$ is given by

$$\mathbf{r} = \mathbf{s} + \mathbf{z}, \tag{3}$$

where $\mathbf{s} = [s_0, \cdots, s_n, \cdots, s_{N-1}]^T = \mathbf{Hx}$ is the channel output, $\mathbf{H}$ is the $N \times N$ circulant matrix of the PLC channel impulse response (CIR), $\mathbf{h} = [h_0, \cdots, h_n, \cdots, h_{N_t-1}]^T$, where N_t is the number of channel taps, and $\mathbf{z} = [z_0, \cdots, z_n, \cdots, z_{N-1}]^T$ is the total PLC noise which consists of AWGN and impulsive noise.

At the receiver, the blanking nonlinear preprocessor bank, $f(\cdot)$, is applied to $\mathbf{r}$, resulting in $\mathbf{y} = [y_0, \cdots, y_n, \cdots, y_{N-1}]^T$. The output of the blanking preprocessor bank is then input to the OFDM demodulator, $\mathbf{Y} = [Y_0, \cdots, Y_k, \cdots, Y_{N-1}]^T = \mathbf{F}f(\mathbf{r})$. The optimal maximum likelihood (ML) bit metric is given by [35]

$$\hat{\mathbf{c}} = \operatorname*{argmin}_{\mathbf{c} \in \mathcal{C}} \sum_{k=0}^{N-1} \sum_{u=1}^{m} \lambda\left(Y_k, c_{k,u}\right), \tag{4}$$

where $\lambda(Y_k, c_{k,u})$ is the bit metric for the u-th bit at the k-th subcarrier given by

$$\lambda\left(Y_k, c_{k,u}\right) = \min_{X_k \in \mathcal{X}^u_{c_{k,u}}} \left| Y_k - G\left(k, k\right) X_k \right|^2, \tag{5}$$

$\mathcal{X}^p_q$ denotes the subset of all the information symbols whose p-th bit has the value of $q \in \{0, 1\}$, and $G(k,k)$ is the k-th diagonal component of $\mathbf{G} = \mathbf{FHF}^H$. The bit metric is then used by the Viterbi decoder to extract the information.

Table 1
PLC Channel Parameters.

Notation	Description	Remark
g_i	gain factor for path i	
a_0 and a_1	attenuation parameters	
ζ	exponent of the attenuation factor	between 0.5 and 1
d_i	length of branch i	
τ_i	delay at branch i	$\tau_i = d_i\sqrt{\epsilon_r}/c_0$
ϵ_r	Dielectric coefficient	
c_0	speed of light	$c_0 = 3 \times 10^8$ m/s

2.1. PAPR reduction technique

In this paper, we use peak amplitude clipping, as discussed in [33]. The peak amplitude clipping block diagram is shown in Fig. 2. Without loss of generality, we set the oversampling factor to be unity.[2]

The OFDM signal is transmitted to the clipping block, which is formulated as

$$\hat{x}_n = \begin{cases} x_n, & |x_n| \leqslant A, \\ 0, & \text{otherwise}, \end{cases} \tag{6}$$

where A is the peak amplitude clipping threshold. The clipping noise is then calculated by subtracting x_n from $\hat{x}_n$. The clipping noise is transformed into the frequency domain, C_k, through FFT. Let $\mathcal{N}$ be the set of indices of null subcarriers, and $\mathcal{N}^c$ be the complement. The following filtering process is then performed as

$$\tilde{C}_k = \begin{cases} C_k, & k \in \mathcal{N}, \\ 0, & k \in \mathcal{N}^c. \end{cases} \tag{7}$$

The time-domain filtered clipping noise signal, $\tilde{c}_n$, is obtained through IFFT. Finally, $\tilde{c}_n$ is summed with x_n to get $\bar{x}_n$. The process can be iterated to suppress the peak regrowth.

2.2. PLC channel model and noise model

The PLC channel can be modeled using the L-path channel model given by [36]

[1] Note that practical PLC standards also employ some null subcarriers.

[2] Oversampling is used to obtain denser discrete-time samples from a continuous-time signal. It is useful to analyze the performance of PAPR reduction. Many papers suggest that the oversampling factor is set at least four to get a more accurate PAPR distribution. As the focus of this paper is not PAPR reduction, i.e., we only show the effect of PAPR reduction on the system performance, we use the unity oversampling factor for the sake of simplicity.

$$H\left(f\right) = \sum_{i=1}^{L} g_i e^{-(a_0+a_1 f^{\zeta})d_i} e^{-j2\pi f\tau_i}, \tag{8}$$

where the variables are defined in Table 1. Also, we normalize the CIR such that $\sum |h_n|^2 = 1$.

As mentioned previously, the total PLC noise consists of AWGN and impulsive noise, i.e. $\mathbf{z} = \mathbf{n} + \mathbf{i}$. The AWGN is a Gaussian vector with mean 0 and variance $2\sigma_n^2$. On the other hand, the impulsive noise is modeled as the Bernoulli-Gaussian process, which mathematically can be expressed as

$$\mathbf{i} = \mathbf{b} \circ \mathbf{g}, \tag{9}$$

where $\mathbf{b}$ is a sequence vector of 1 and 0 with a probability of p and $1-p$, respectively, $\mathbf{g}$ is a vector of AWGN with mean 0 and variance of $2\sigma_g^2$, and '$\circ$' denotes the Hadamard product. The impulsive noise is characterized by a signal-to-impulsive noise ratio given by $SINR = 1/2\sigma_g^2$.

2.3. Proposed blanking preprocessor bank

The blanking preprocessor bank consists of Q blanking preprocessors with different thresholds. Each blanking preprocessor is denoted by $y_n^q = f_q(\cdot)$, where $q = 1, \cdots, Q$, and given by

$$y_n^q = \begin{cases} r_n, & |r_n| \leqslant T_q, \\ 0, & \text{otherwise}, \end{cases} \tag{10}$$

To better analyze the nonlinear preprocessing characteristic, a linearized form is commonly used as follows

$$y_n^q = \alpha_q s_n + d_n, \tag{11}$$

where α_q is a real-valued constant chosen such that $E[d_n s_n^*] = 0$, '$*$' is the complex conjugate operator and $E[\cdot]$ denotes expectation, and d_n can be considered as the blanking noise. Note that it is preferred to carefully choose the threshold such that $\alpha_q \approx 1$ [18]. The constant α_q is defined by $\alpha_q = E[y_n^{q^*} s_n]$. As a nonlinear preprocessor processes the blanking operation on an OFDM symbol level, in practice, we can approximate α_q for each blanking block with $\alpha_q = 1 - N_B^q/N$, where N_B^q is the number of blanked samples in the q-th preprocessor [37]. This way, the preprocessor does not need the knowledge of the noise or transmit signal statistics.

It is obvious that (11) is similar to the received signal in multiple fading paths. Further, the output SNR of each blanking preprocessor can be calculated by

$$\begin{aligned} \gamma_q &= \frac{E\left[\left|\alpha_q s_n\right|^2\right]}{E\left[\left|y_n^q - \alpha_q s_n\right|^2\right]} \\ &= \left(\frac{E\left[\left|y_n^q\right|^2\right]}{\alpha_q^2} - 1\right)^{-1}. \end{aligned} \tag{12}$$

Note that $E[|s_n|^2] = 1$ as assumed previously.

The output of the blanking preprocessor bank is given by

$$y_n = \sum_{q=1}^{Q} w_q y_n^q, \tag{13}$$

where w_q is the weight for q-th preprocessor. Using the maximal ratio combining (MRC) scheme, optimal performance can be obtained by setting $w_q = \alpha_q$.

3. Simulation results

In this paper, we use a BICM OFDM PLC system with QPSK modulation, the number of subcarriers is $N = 512$, and only $K = 480$ subcarriers carry data. Without loss of generality, we assume the null subcarriers are located at low frequencies. The convolutional codes are used with code rate 1/2 and generator polynomial $[171, 133]_8$. The number of iterations of the peak amplitude clipping and the corresponding threshold is chosen to be $j = 1$ and $A = 1.2$, respectively, as presented in [33]. The PLC channel parameters are given in Table 2 [36].

Table 2
PLC channel parameters for real-world networks.

Path No	1	2	3	4
d_i (m)	150	188	264	397
g_i	0.4	−0.4	−0.8	−1.5
$\zeta = 0.5$, $a_0 = 0$, $a_1 = 8 \times 10^{-6}$, $\epsilon_r = 4$				

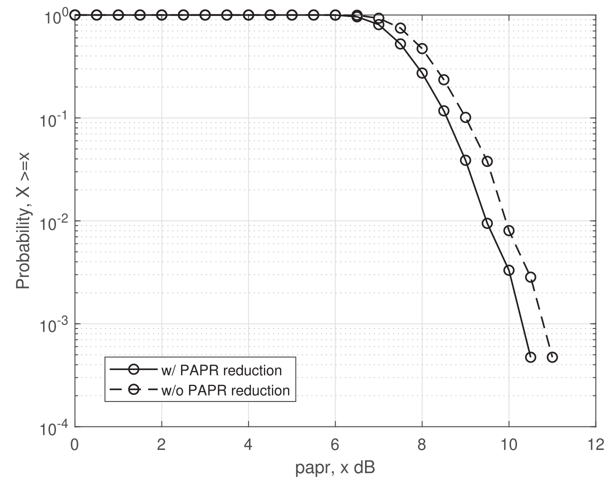

Fig. 3. PAPR performance.

We analyze the PLC system using our proposed blanking preprocessor bank in two scenarios. In the first scenario, the impulsive noise parameters are fixed, i.e. $p = 0.01, SINR = -10$ dB. On the other hand, we vary the impulsive noise parameters in the second scenario to observe our proposed blanking method's robustness. The probability of impulsive noise is set as a random variable following a uniform distribution on the interval of 0.005 to 0.02. Similarly, the SINR also follows uniform distribution on the interval −5 dB to −15 dB. The thresholds for the proposed blanking preprocessor bank are selected as follows. The thresholds are given by $\{T\} = \{T_l + (i-1)\Delta T\}_{i=1}^{Q}$. The lower limit of the threshold is set at $T_l = 2.0$, and the higher limit of the threshold is set at $T_h = 3.0$. The threshold steps are set to be $\Delta T = 0.05$ and $\Delta T = 0.2$, which means $Q = 21$ and $Q = 6$, respectively. We then sort the preprocessor outputs based on the α_q values. Subsequently, we take 100%, 80%, and 50% of preprocessor outputs with the highest α_q values to be combined. Keep in mind that we want the preprocessor outputs with $\alpha_q \approx 1$. In other words, we combine the best 21, 16, and 10 preprocessor outputs for $\Delta T = 0.05$ and 6, 4, and 3 outputs for $\Delta T = 0.2$.

It is worth mentioning that the selection of T should be arbitrary. However, keep in mind that the lower threshold will cause information loss, and a higher threshold will make many large samples left unblanked. The reasonable values of the threshold are between 2.0 and 3.5 based on the dynamic range of the OFDM signal amplitude. On the other hand, the value of Q is determined by the threshold step selection, ΔT, which can be chosen between 0.05 and 0.2 and depends on the range of T. The rule of thumb is when the range of T is large, smaller Q can be assigned, and vice versa.

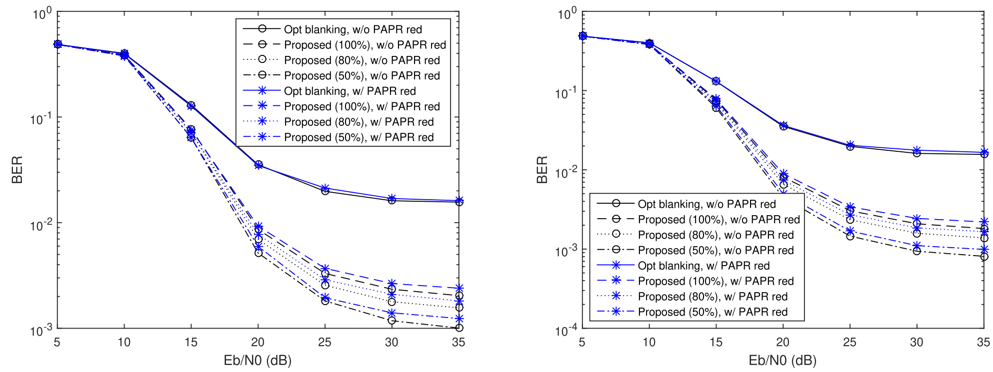

(a) $\Delta T = 0.05$ (b) $\Delta T = 0.2$

Fig. 4. BER performance, $p = 0.01, SINR = -10$ dB.

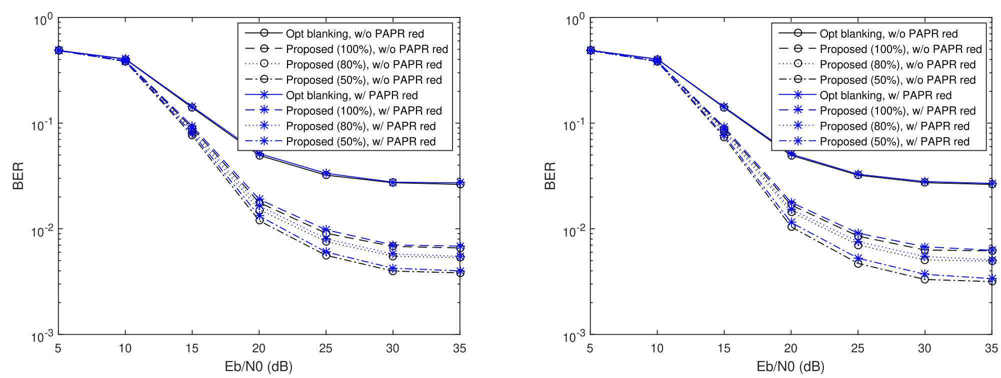

(a) $\Delta T = 0.05$ (b) $\Delta T = 0.2$

Fig. 5. BER performance, random p and $SINR$.

3.1. PAPR performance

PAPR is commonly analyzed using complementary cumulative distribution function (CCDF), which shows the probability of PAPR exceeds a certain level. The CCDF plot of the proposed system is shown in Fig. 3. It can be seen that the PAPR is reduced by about 0.5 dB at a probability of 10^{-3}. It is worth mentioning that the gain of our PAPR reduction method is proportional to the number of null subcarriers, i.e., the more the null subcarriers, the more the PAPR reduction.

3.2. BER performance

The BER performance of the PLC system with the optimal blanking and the proposed blanking, along with and without peak amplitude clipping, for $\Delta T = 0.05$ and $\Delta T = 0.2$ is shown in Figs. 4a and b, respectively. It can be observed from the two figures that the BER performance for the proposed blanking outperforms one of the optimal blankings. Note that the optimum threshold is obtained by optimizing the output SNR as $\min_T (E[|y_n|^2])/\alpha$, where the closed-form expressions of $E[|y_n|^2]$ and α for blanking nonlinearity are given in [18].

The results are understandable as some useful information is missing due to the optimal blanking. On the contrary, the missing information can be retrieved through multiple outputs (or "blanking channels") in the proposed blanking scheme. It can also be seen that the BER plots of the proposed blanking are relatively the same for 100%, 80%, and 50% schemes. Further, increasing ΔT from 0.05 to 0.2 shows little effect on the performance.

BER performance for random impulsive noise parameters $\Delta T = 0.05$ and $\Delta T = 0.2$ is shown in Figs. 5a and b. It can be seen that the BER plots for the proposed blanking are significantly better compared with one of the optimal blanking. Further, it can be seen that the peak amplitude clipping relatively does not deteriorate the BER performance. It is because the peak amplitude clipping is performed in the null subcarriers and $\mathcal{N} \cup \mathcal{N}^c = \emptyset$.

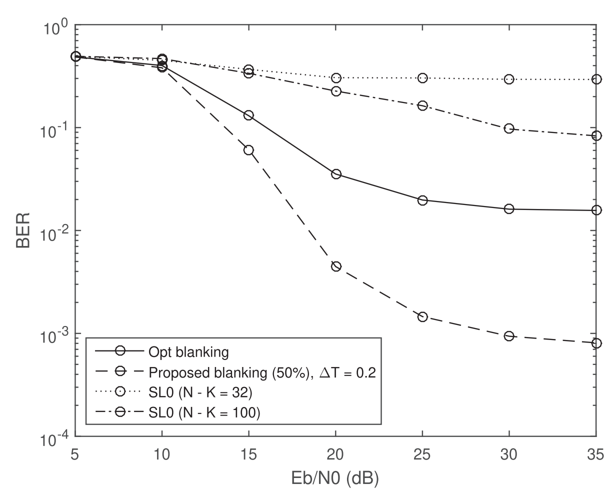

Fig. 6. BER performance comparison.

As we use null subcarriers, it is worth to compare the BER performance of the blanking method with the compressive sensing method. We employ SL0 as the impulsive noise reconstruction algorithm. The procedure of impulsive noise reconstruction and mitigation follows

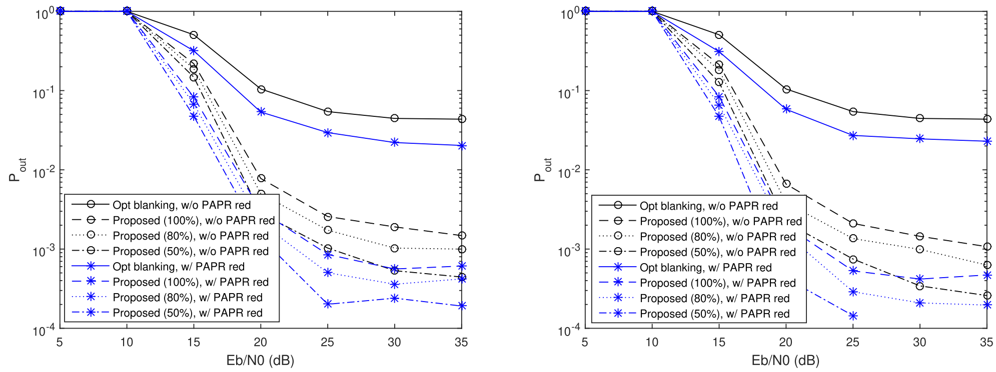

(a) $\Delta T = 0.05$ (b) $\Delta T = 0.2$

Fig. 7. Outage probability, $p = 0.01, SINR = -10$ dB.

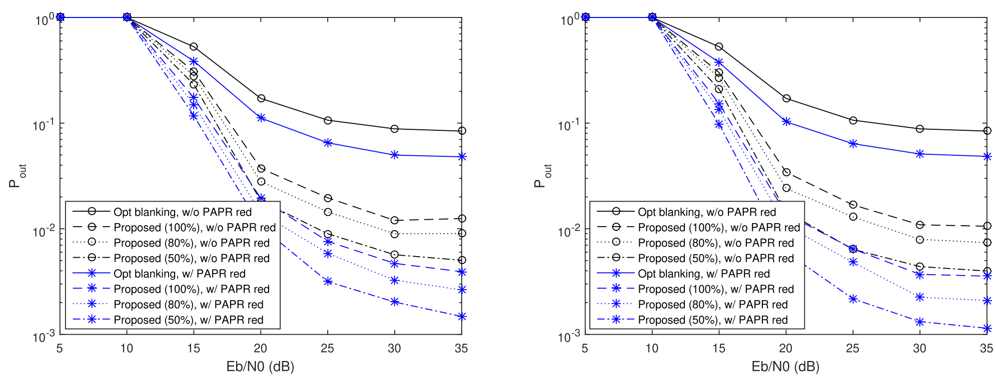

(a) $\Delta T = 0.05$ (b) $\Delta T = 0.2$

Fig. 8. Outage probability, random p and $SINR$.

[33]. We choose the SL0 algorithm since it has low complexity and performs better than the ℓ_1 algorithm [38,23]. The BER plots are depicted in Fig. 6. It can be seen that using the same number of null subcarriers ($N - K = 32$), the clipping method yields better performance. Compressive sensing performance depends on the number of null subcarriers. In general, the more null subcarriers, the better the performance. Therefore, in order to obtain good performance, it needs to sacrifice the data rate.

3.3. Outage probability

Outage probability can be used as a metric to measure the system performance related instantaneous output SNR of the blanking preprocessor(s). It is defined as the probability of mutual information, I less than the information rate, R [39]. Mathematically, it can be written as

$$\begin{aligned} P_{out} &= \Pr(I < R) \\ &= \Pr(\log_2(1+\gamma) < R) \\ &= \Pr(\gamma < 2^R - 1), \end{aligned} \tag{14}$$

where γ is the output SNR of the blanking preprocessor bank.

In this paper, we use $R = 3$. The outage probability plot with varying SNR with fixed impulsive noise parameters for $\Delta T = 0.05$ and $\Delta T = 0.2$ is depicted in Figs. 7a and b. It can be seen that the outage probability for the system with the blanking preprocessor bank outperforms the one

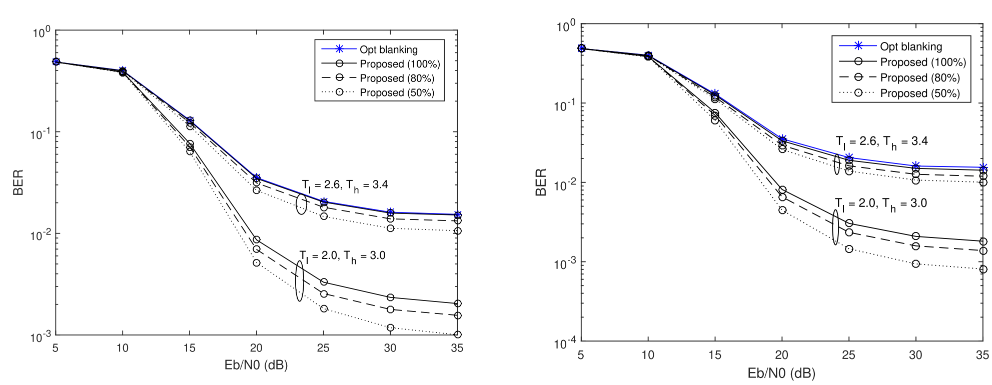

(a) $\Delta T = 0.05$ (b) $\Delta T = 0.2$

Fig. 9. BER plots, $p = 0.01$ and $SINR = -10$ dB.

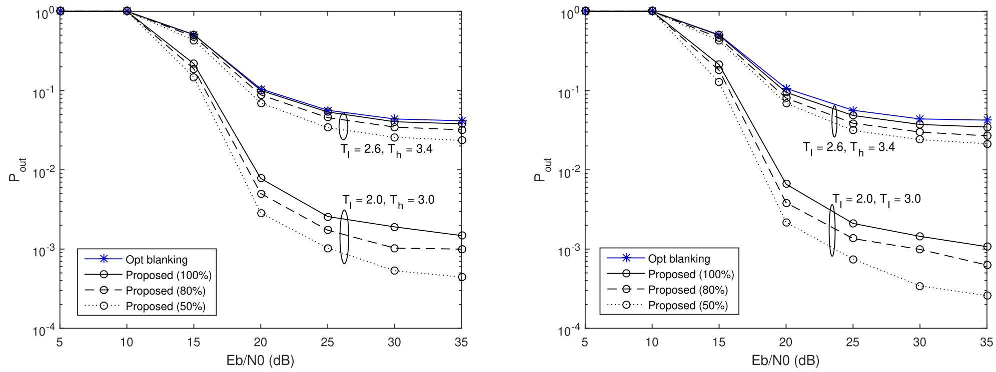

(a) $\Delta T = 0.05$ (b) $\Delta T = 0.2$

Fig. 10. Outage probability, $p = 0.01$ and $SINR = -10$ dB.

with optimal blanking. We further observe that the outage probability becomes better when combining a smaller portion of the blanking preprocessors.

Figs. 8a and b show the outage probability for random impulsive noise parameters for $\Delta T = 0.05$ and $\Delta T = 0.2$, respectively. The general trends show the robustness of our proposed method compared to the optimal blanking. Further, we can observe that the PAPR reduction technique plays an important role in reducing the blanker's false alarm. As a result, the outage probabilities are reduced.

The blanking process for our proposed scheme has the same complexity as the optimal blanking scheme, i.e., $\mathcal{O}(N)$. Our proposed method needs to perform a sorting algorithm, which gives an additional complexity of $\mathcal{O}(Q\log Q)$. This may have an effect on the computation time. However, in the optimal blanking scheme, we have an additional complexity for calculating the optimum threshold (although it can be estimated offline).

3.4. Effect of thresholds selection

The performance of our proposed method depends on the threshold selection of the blanking nonlinear preprocessors. To analyze the effect of the threshold selection, we provide the second threshold setting, i.e. $T_l = 2.6$ and $T_h = 3.4$, with the same ΔT. We then compare the performance with the first (previous) threshold setting.

Figs. 9a and b show the comparison of BER plots using two different threshold sets for $\Delta T = 0.05$ and $\Delta T = 0.2$, respectively. It can be seen that using the second threshold setting gives performance degradation in both BER and outage performance. It may be caused by improper setting of the higher limit of threshold (too large) in the second set so that most of the samples are left unblanked. Moreover, we notice that BER and outage probability plots of the 100% scheme for the second threshold set are close to the optimal blanking plots. This can be explained as follows. When the thresholds are not properly set, poor outputs from a few blanking preprocessors may occur. They may degrade the overall performance. However, the poor outputs' adverse effects can be eliminated by taking 80% and 50% of the best output. That's why the 80% and 50% schemes result in better performance compared with the optimal blanking scheme. Likewise, Figs. 10a and b shows the outage probability plots with similar trends.

4. Conclusion and future work

We have proposed a blanking preprocessor blank, which consists of multiple blanking preprocessors with different thresholds. The proposed method does not need prior information about the impulsive noise. However, the threshold selection should be carefully considered. This means that the lower and higher limit of thresholds should not be set too small and large, respectively. It has been shown through simulations that the proposed method, in terms of BER and outage probability, outperforms one of the optimal blankings, even when we take only 50% of the best values. The advantages of our proposed scheme are: (1) optimal threshold does not need to be calculated and (2) assurance of obtaining improved performance (compared with the optimum threshold) by processing 80% or 50% of the best blanking preprocessor outputs. The drawbacks of our blanking bank preprocessor are (1) selection of thresholds should be considered carefully, and (2) there is some extra computation time. Further, our proposed scheme can be implemented in other OFDM-based PLC, such as WT-OFDM. We will perform the analysis of its performance as our future work.

Declaration of Competing Interest

The authors declare that they have no known competing financial interests or personal relationships that could have appeared to influence the work reported in this paper.

Acknowledgment

This work was supported by Fundamental Research Grant Scheme (FRGS) from the Ministry of Higher Education Malaysia under FRGS/1/2016/TK04/CURTIN/02/1.

References

[1] Padhan AK, Sahu PR, Samantaray SR. Performance of smart grid dynamic HAN with RQAM and GMSK modulation. IEEE Commun Lett 2019;23(11):1940–3.
[2] Zhang L, Kerrigan EC, Pal BC. Optimal communication scheduling in the smart grid. IEEE Trans Ind Inform 2019;15(9):5257–65.
[3] Galli S, Scaglione A, Wang Z. For the grid and through the grid: The role of power line communications in the smart grid. Proc IEEE 2011;99(6):998–1027.
[4] Cataliotti A, Cara DD, Fiorelli R, Tiné G. Power-line communication in medium-voltage system: Simulation model and onfield experimental tests. IEEE Trans Power Del 2012;27(1):62–9.
[5] Yoon S-G, Jang S, Kim Y-H, Bahk S. Opportunistic routing for smart grid with power line communication access network. IEEE Trans Smart Grid 2014;5(1):303–11.
[6] Tonello A, Pittolo A. Considerations on narrowband and broadband power line communication for smart grids. In: Proc IEEE SmartGridCom, Miami, FL, USA; 2015. p. 13–8.
[7] Shrestha D, Mestre X, Payaro M. On channel estimation for power line communication systems in the presence of impulsive noise. Comput Electr Eng 2018;72:406–19.
[8] Bai L, Tucci M, Raugi M. Impulsive noise mitigation with interleaving based on MUSIC in power line communication. IEEE Trans Smart Grid 2019;10(4):3575–84.
[9] Andreadou N, Pavlidou F-N. Modelling the noise on the OFDM power-line communications systems. IEEE Trans Power Del 2010;25(1):150–7.
[10] Meng H, Guan YL, Chen S. Modeling and analysis of noise effects on broadband power-line communications. IEEE Trans Power Del 2005;20(2):630–7.
[11] Ndo G, Siohan P, Hamon M-H. Adaptive noise mitigation in impulsive environment: Application to power-line communications. IEEE Trans Power Del 2010;25(2):647–56.
[12] Ghosh M. Analysis of the effect of impulse noise on multicarrier and single carrier QAM systems. IEEE Trans Commun 1996;44(2):145–7.

[13] Lin J, Nassar M, Evans BL. Impulsive noise mitigation in powerline communications using sparse bayesian learning. IEEE J Select Areas Commun 2013;31(7):1183–972.
[14] Andreadou N, Fulli G. NB-PLC channel: Estimation of periodic impulsive noise parameters and mitigation techniques. Int J Elec Power Energy Syst 2018;103:146–58.
[15] Chien Y, Yu H. Mitigating impulsive noise for wavelet-OFDM powerline communication. Energies 2019;12(8):1–13.
[16] Yu H, Chien Y, Tsao H. A study of impulsive noise immunity for wavelet-OFDM-based power line communications. In: Proc Int Conf Commun Problem-Solving, Taipei, Taiwan; 2016. p. 1–2.
[17] Mariyam PD, Juwono FH, Pamungkasari PD, Gunawan D. How to deal with impulse noise in OFDM-based PLC: A survey. In: Proc IEEE Int Elect Eng Inform, Banda Aceh, Indonesia; 2017. p. 163–8.
[18] Juwono FH, Guo Q, Huang D, Wong KP. Deep clipping for impulsive noise mitigation in OFDM-based power-line communications. IEEE Trans Power Del 2014;29(3):1335–43.
[19] Rabie KM, Alsusa E. Performance analysis of adaptive hybrid nonlinear preprocessors for impulsive noise mitigation over power-line channels. In: Proc IEEE Int Conf Commun, London, UK; 2015. p. 728–33.
[20] Chien Y. Iterative channel estimation and impulsive noise mitigation algorithm for OFDM-based receivers with application to power-line communications. IEEE Trans Power Del 2015;30(6):2435–42.
[21] Mao M, Xie G, Gao J, Wu G, Liu K. Adaptive IN mitigation in OFDM-based power-line communication system with jointed blanking and robust channel estimation. In: Proc IEEE Int Conf Comput Commun, Chengdu, China; 2016. p. 2573–6.
[22] Chien Y, Chen J, Xu SS. A multilayer perceptron-based impulsive noise detector with application to power-line-based sensor networks. IEEE Trans Power Del 2018;6:21778–87.
[23] Juwono FH, Guo Q, Huang D, Wong K, Xu L. Impulse noise detection in PLC with smoothed L0-norm. In: Proc IEEE Int Acoust Speech Signal Process, Brisbane, Australia; 2015. p. 3232–6.
[24] Ren G, Qiao S, Hei Y. Asynchronous impulsive noise mitigation in OFDM using adaptive threshold compressive sensing. In: Proc Wireless Microwave Technol Conf, Tampa, FL, USA; 2014. p. 1–5.
[25] Adebisi B, Anoh K, Rabie KM, Ikpehai A, Fernando M, Wells A. A new approach to peak threshold estimation for impulsive noise reduction over power line fading channels. IEEE Syst J 2019;13(2):1682–93.
[26] Juwono FH, Guo Q, Huang D, Chen Y, Xu L, Wong KP. On the performance of blanking nonlinearity in real-valued OFDM-based PLC. IEEE Trans Smart Grid 2018;9(1):449–57.
[27] Juwono FH, Reine R, Liu L, Liu J, Huang D. Performance of impulsive noise blanking in precoded OFDM-based PLC systems. In: Proc Int Conf Commun Syst, Shenzhen, China; 2016. p. 1–6.
[28] Fang F, Yang Z. Improved blanking nonlinearity scheme for powerline communication system in impulsive noise scenarios. In: Proc IEEE Int Conf Comput Commun Internet, Wuhan, China; 2016. p. 70–5.
[29] Alsusa E, Rabie KM. Dynamic peak-based threshold estimation method for mitigating impulsive noise in power-line communication systems. IEEE Trans Power Del 2013;28(4):2201–8.
[30] Rabie KM, Alsusa E. Improving blanking/clipping based impulsive noise mitigation over powerline channels. In: Proc IEEE Int Symp Pers Indoor Mobile Radio Commun., London, UK; 2013. p. 3413–7.
[31] Kageyama T, Muta O, Gacanin H. Enhanced selected mapping for impulsive noise blanking in multi-carrier power-line communication systems. IEICE Trans Commun 2019;E102B(11):2174–82.
[32] Rabie KM, Alsusa E. Effective noise cancellation using single-carrier FDMA transmission in power-line channels. IEEE Trans Power Del 2014;29(5):2110–7.
[33] Juwono FH, Guo Q, Huang D, Wong KP. Joint peak amplitude and impulsive noise clippings in OFDM-based power line communications. In: Proc. Asia Pacific Conf. Commun.; 2013. p. 567–71.
[34] Juwono FH, Reine R, Liu J, Pamungkasari PD. BITFCM-OFDM scheme for power-line communication systems. AEU - Int J Electron Commun 2019;105:116–23.
[35] Huang D, Letaief KB, Lu J. Bit-interleaved time-frequency coded modulation for OFDM systems over time-varying channels. IEEE Trans Commun 2005;53(7):1191–9.
[36] Zimmermann M, Dostert K. A multi-path signal propagation model for the power line channel in the high frequency range. In: Proc int symp power line communications and its applications; 1999. p. 45–51.
[37] Epple U, Shibli K, Schnell M. Investigation of blanking nonlinearity in OFDM systems. In: Proc int conf commun, Kyoto, Japan; 2011. p. 1–5.
[38] Mohimani H, Babaie-Zadeh M, Jutten C. A fast approach for overcomplete sparse decomposition based on ℓ^0 norm. IEEE Trans Signal Process 2009;57(1):289–301.
[39] Mathur A, Ai Y, Cheffena M, Bhatnagar MR. Performance of hybrid ARQ over power line communications channels. In: Proc IEEE 91st Vehi Technol Conf, Antwerp, Belgium; 2020. p. 1–6.